Molecular Crystals and Liquid Crystals Science and Technology. Section A. Molecular Crystals and Liquid Crystals

Publication details, including instructions for authors and subscription information:
http://www.tandfonline.com/loi/gmcl19

Coupling of Electrons To Low-Frequency Phonons in Cation Radical Salts of TTF Studied by Resonance Raman Scattering

Adolfo Speghini [a] , Danilo Pedron [a] , Carlo Bellitto [b] , Luigino Feltre [b] & Renato Bozio [b]

[a] Department of Physical Chemistry, University of Padova, via Loredan 2, 1-35131, Padova, Italy

[b] I.T.S.E., C.N.R., Area della Ricerca di Roma, C.P. 10, Via Salaria km. 29.5, 1-00016, Monterotondo Staz, Roma

Version of record first published: 04 Oct 2006.

To cite this article: Adolfo Speghini , Danilo Pedron , Carlo Bellitto , Luigino Feltre & Renato Bozio (1993): Coupling of Electrons To Low-Frequency Phonons in Cation Radical Salts of TTF Studied by Resonance Raman Scattering, Molecular Crystals and Liquid Crystals Science and Technology. Section A. Molecular Crystals and Liquid Crystals, 234:1, 219-226

To link to this article: http://dx.doi.org/10.1080/10587259308042919

Mol. Cryst. Liq. Cryst. 1993, Vol. 234, pp. 219–226
Reprints available directly from the publisher
Photocopying permitted by license only

Printed in the United States of America

COUPLING OF ELECTRONS TO LOW-FREQUENCY PHONONS IN CATION RADICAL SALTS OF TTF STUDIED BY RESONANCE RAMAN SCATTERING

ADOLFO SPEGHINI[‡], DANILO PEDRON[‡], CARLO BELLITTO[§], LUIGINO FELTRE[‡] and RENATO BOZIO[‡]
[‡] Department of Physical Chemistry, University of Padova, via Loredan 2, I-35131 Padova, Italy. [§] I.T.S.E., C.N.R., Area della Ricerca di Roma, C.P. 10, Via Salaria km. 29.5, I-00016 Monterotondo Staz. (Roma).

Abstract We report results obtained by measuring the low frequency (40–150 cm^{-1}) resonance Raman scattering (RRS) spectra and excitation profiles of the cation radical salt $(TTF)_2(W_6O_{19})$ whose structure consists of almost isolated $(TTF^+)_2$ dimers that are characterized by a CT absorption band at 850 nm. Quantitative analysis of the RRS data has been performed based on a Peierls–Hubbard model for an isolated dimer. The parameters required for the calculation of the RRS data are derived analytically from the microscopic parameters of the Peierls–Hubbard Hamiltonian, which include the intermolecular (EIP) coupling constants. The excitation profiles have been calculated using the time correlator technique and their fitting provides the first experimental estimates of the EIP coupling constants.

INTRODUCTION

The coupling of electrons with molecular motions plays a central role in numerous chemical and physical phenomena. Examples range from electrochemical and photoinduced electron transfer processes to macroscopic charge transport and electronically driven structural transitions (e.g., the Peierls transition) in molecular conducting materials and, possibly, to the onset of organic superconductivity [1]. In molecular materials, electrons can couple both with intramolecular vibrational modes and with translational and librational motions of the molecule as a whole. The former modes are effective in modulating the orbital energy ϵ whereas coupling with the intermolecular modes occurs because of their ability to modulate the electron hopping integrals t [2]. This type of coupling becomes particularly relevant in systems containing closely spaced molecular entities that exhibit comparatively strong charge transfer (CT) interactions. While a fair amount of knowledge has been accumulated on the electron–molecular vibration (EMV) interactions in CT crystals and molecular conductors [2], effective experimental means of investigating the electron–intermolecular phonon (EIP) couplings are still under development.

A method based on the analysis of the Raman scattering intensities of low frequency intermolecular modes measured with exciting laser wavelengths in

resonance with the CT transition is presented in this work. The theoretical analysis is based on a calculation of the resonance Raman scattering (RRS) properties of a Peierls–Hubbard Hamiltonian for the simplest possible system consisting of two molecular sites with two electrons [3]. The method is experimentally demonstrated by reporting and analysing the RRS spectra and excitation profiles of the cation radical salt $(TTF)_2(W_6O_{19})$ containing almost isolated $(TTF^+)_2$ dimers. Experimental estimates of the EIP coupling constants, of the hopping integral and of the on–site correlation energy are thereby obtained and compared with previous knowledge.

THEORY

Our model represents a dimer of two identical molecular radicals (labeled 1 and 2) using a two–sites, two–electrons Peierls–Hubbard hamiltonian, which reads

$$H = H_E + H_{EV} + H_V = H_E + H_{EMV} + H_{EIP} + H_V. \tag{1}$$

Denoting as t the electron transfer interaction and U the on–site electron correlation, the electronic Hamiltonian is

$$H_E = -t\sum_{\sigma}(a^{\dagger}_{1,\sigma}a_{2,\sigma} + a^{\dagger}_{2,\sigma}a_{1,\sigma}) + U(n_{1\uparrow}n_{1\downarrow} + n_{2\uparrow}n_{2\downarrow}) = \sum_{n=1}^{6} E_n A^{\dagger}_n A_n. \tag{2}$$

The eigenstate creation operators $(A^{\dagger}_n)$ and eigenvalues (E_n) of H_E are given in Table 1.

TABLE 1 Eigenvectors and eigenvalues of the Hubbard dimer Hamiltonian.

Basis states	Eigenvector	Eigenvalues
$\|S_0\rangle = \frac{1}{\sqrt{2}}(a^{\dagger}_{1\uparrow}a^{\dagger}_{2\downarrow} + a^{\dagger}_{2\uparrow}a^{\dagger}_{1\downarrow})\|0\rangle$	$\|1\rangle = b_1\|S_0\rangle + c_1\|CT_+\rangle = A^{\dagger}_1\|0\rangle$	$E_1 = E_-$
$\|CT_\pm\rangle = \frac{1}{\sqrt{2}}(a^{\dagger}_{1\uparrow}a^{\dagger}_{1\downarrow} \pm a^{\dagger}_{2\uparrow}a^{\dagger}_{2\downarrow})\|0\rangle$	$\|2\rangle = b_2\|S_0\rangle + c_2\|CT_+\rangle = A^{\dagger}_2\|0\rangle$	$E_2 = E_+$
$\|T_1\rangle = a^{\dagger}_{1\uparrow}a^{\dagger}_{2\uparrow}\|0\rangle$	$\|3\rangle = \|CT_-\rangle = A^{\dagger}_3\|0\rangle$	$E_3 = U$
$\|T_0\rangle = \frac{1}{\sqrt{2}}(a^{\dagger}_{1\uparrow}a^{\dagger}_{2\downarrow} - a^{\dagger}_{2\uparrow}a^{\dagger}_{1\downarrow})\|0\rangle$	$\|4\rangle = \|T_1\rangle = A^{\dagger}_4\|0\rangle$	$E_4 = 0$
$\|T_{-1}\rangle = a^{\dagger}_{1\downarrow}a^{\dagger}_{2\downarrow}\|0\rangle$	$\|5\rangle = \|T_0\rangle = A^{\dagger}_5\|0\rangle$	$E_5 = 0$
	$\|6\rangle = \|T_{-1}\rangle = A^{\dagger}_6\|0\rangle$	$E_6 = 0$
$b_{1,2} = [1 + (E_{1,2}/2t)^2]^{-\frac{1}{2}}$	$b^2_{1,2} + c^2_{1,2} = 1$	$E_\pm = \frac{1}{2}(U \pm \sqrt{U^2 + 16t^2})$

The purely vibrational part of H reads

$$H_V = \sum_i \frac{\hbar\omega_i}{4}(P^2_{1i} + P^2_{2i} + Q^2_{1i} + Q^2_{2i}) + \sum_e \frac{\hbar\omega_e}{4}(v^2_e + u^2_e) \tag{3}$$

where Q_{ni}, P_{ni}, ω_i are the dimensionless coordinate and momentum and the angular frequency of the ith intramolecular mode of the nth molecule, while u_e, v_e, ω_e have the corresponding meanings for the intermolecular (external) modes. The electron–vibration interaction Hamiltonian H_{EV} includes an electron–intramolecular vibration (EMV) coupling term

$$\begin{aligned} H_{EMV} &= \sum_i 2^{-1/2} g_i q_i (n_1 - n_2) \\ &= \sum_i V_{13}(i) q_i (A_1^\dagger A_3 + A_3^\dagger A_1) + \sum_i V_{23}(i) q_i (A_2^\dagger A_3 + A_3^\dagger A_2) \end{aligned} \tag{4}$$

and an electron–intermolecular phonon (EIP) coupling term

$$\begin{aligned} H_{EIP} &= -\sum_e g_e u_e \sum_\sigma (a_{1,\sigma}^\dagger a_{2,\sigma} + a_{2,\sigma}^\dagger a_{1,\sigma}) \\ &= \sum_e P_{11}(e) u_e (A_1^\dagger A_1) + \sum_e P_{22}(e) u_e (A_2^\dagger A_2) + \sum_e P_{12}(e) u_e (A_1^\dagger A_2 + A_2^\dagger A_1). \end{aligned} \tag{5}$$

In Eq. (4), $q_i = 2^{-1/2}(Q_{1i} - Q_{2i})$ are the dimer modes corresponding to the anti–symmetric coupling of the intramolecular vibrational coordinates. The strength of the linear EMV and EIP coupling is specified by $g_i = (\partial\epsilon/\partial Q_i)_0$ and $g_e = (\partial t/\partial u_e)_0$, respectively, and by the following definitions of the coupling constants, defined on the basis of the electronic eigenstates $|n\rangle$ (n = 1,2,3)

$$\begin{aligned} &V_{13}(i) = 2^{1/2} c_1 g_i \quad ; \quad V_{23}(i) = 2^{1/2} c_2 g_i \\ &P_{11}(e) = -4 b_1 c_1 g_e \quad ; \quad P_{22}(e) = -4 b_2 c_2 g_e \quad ; \quad P_{12}(e) = -2(b_1 c_2 + b_2 c_1) g_e. \end{aligned}$$

For the dimer at equilibrium the dipole moment operator is

$$\begin{aligned} \mu &= -\frac{1}{2} e d (n_1 - n_2) = -ed[c_1 (A_1^\dagger A_3 + A_3^\dagger A_1) + c_2 (A_2^\dagger A_3 + A_3^\dagger A_2)] \\ &= \mu_{13} (A_1^\dagger A_3 + A_3^\dagger A_1) + \mu_{23} (A_2^\dagger A_3 + A_3^\dagger A_2) \end{aligned} \tag{6}$$

where d is the spacing between radicals in the dimer.

From Eqs. (4) and (5) one sees that the crude adiabatic states $|n\rangle = A_n^\dagger |0\rangle$, solutions of the electronic term H_E, are not eigenstates of H_{EV}. Approximate electronic eigenstates can be written as Herzberg–Teller (HT) adiabatic wavefunctions [4]

$$|\, n^{HT}(\{q_i, u_e\})\rangle = |\, n\rangle + \sum_{m \neq n} \frac{(H_{EV})_{mn}}{E_n - E_m} |\, m\rangle. \tag{7}$$

The fact that several modes can couple with the same pair of states implies frequency shifts and mode mixing (Duschinsky rotation) [5] of the normal coordinates. This is easily seen when one considers that the total harmonic potential energy

$$E_n^{HT}(\{q_i, u_e\}) = E_n + (H_{EV})_{nn} + \sum_i \frac{\hbar\omega_i}{4} q_i^2 + \sum_e \frac{\hbar\omega_e}{4} u_e^2 + \sum_{k \neq n} \frac{(H_{EV})_{nk}(H_{EV})_{kn}}{E_n - E_k} \tag{8}$$

contains products of vibronic matrix elements. From this equation one can also note that terms such as $P_{11}(e)$ and $P_{22}(e)$, diagonal in the electronic state index, originate displacements of the minima of the potential energies.

Note that all the energies and matrix elements appearing in Eqs. (7) and (8), as well as the transition dipole matrix elements between the HT states, Eq. (7), can be calculated analytically from the fundamental parameters of the Peierls–Hubbard Hamiltonian, namely t, U, $\{g_i\}$ and $\{g_e\}$.

The spontaneous Raman differential scattering cross section $\sigma_R(\omega_L,\omega_S)$ in the rotating wave approximation is given by [6,7]

$$\sigma_R = C\ \omega_L\omega_S^3\ \Re\{\int_0^\infty dt_3 \int_0^\infty dt_2 \int_0^\infty dt_1\ R(t_3,t_2,t_1)\ e^{-i\omega_L t_1 - i(\omega_L-\omega_S)t_2 + i\omega_S t_3}\} \tag{9}$$

where C is a numerical constant, $\Re\{z\}$ indicates the real part of z and the third order non–linear response function in the time domain $R(t_3,t_2,t_1)$ can be written in term of a four–point correlation function of the dipole moment operator

$$R(t_3,t_2,t_1) = \langle\mu(\tau_1)\mu(\tau_2)\mu(\tau_3)\mu(\tau_4)\rangle \equiv Tr[\mu(\tau_1)\mu(\tau_2)\mu(\tau_3)\mu(\tau_4)\rho^{(0)}] \tag{10}$$

where τ_i represents an appropriate combination of the t_i variables, $\rho^{(0)}$ represents the thermal equilibrium density matrix and $\mu(t) = e^{-iHt}\ \mu\ e^{iHt}$. The trace is performed over the complete set of eigenstate of the system.

Approximating the Peierls–Hubbard Hamiltonian as diagonal in the HT states (cfr. Eqs. (7) and (8))

$$H \simeq \sum_n |\, n^{HT}\rangle E_n^{HT} \langle n^{HT}\,| \quad ,$$

assuming that the thermal bath generates homogeneous bands in the spectra, one can perform the calculation of R from the knowledge of the energies E_n^{HT} and the transition dipole matrix elements between the HT states.

For a symmetric dimer possessing inversion symmetry, all three anti–phase combinations of the rigid translational motions of the two molecules belong to the *gerade* symmetry and are therefore expected to be Raman active. These modes modulate effectively the transfer integral so that they exhibit non–zero coupling constants $\{g_e\}$. This modulation provides an efficient mechanism for intensity enhancement at resonance with the CT transition. No such mechanism is operative for the intramolecular vibrational modes.

EXPERIMENTAL RESULTS AND DISCUSSION

In choosing a system suitable for experimental investigations we have used the following criteria. (i) The crystal structure is made up of dimeric units with negligible CT interaction among them; (ii) the molecular constituents are key components of organic conductors and superconductors; (iii) the CT absorption band lies at wavelengths accessible to the available laser sources. Previous RRS results have been reported for the crystalline cation radical salt (TTF)Br [3] which

satisfies the above requirements except for the fact that it has a very large unit cell containing eight formula units [8]. Raman spectra in resonance with the CT band were obtained using only three lines of a kripton laser.

In the present work we shall report new results on $(TTF)_2(W_6O_{19})$ which has two formula units (hence two dimers) per unit cell [9]. Another important difference with respect to (TTF)Br is the much heavier mass of the counter-anions bearing a (2–) charge. This should imply a large difference in the possible coupling between intermolecular modes of the dimer and anion motions.

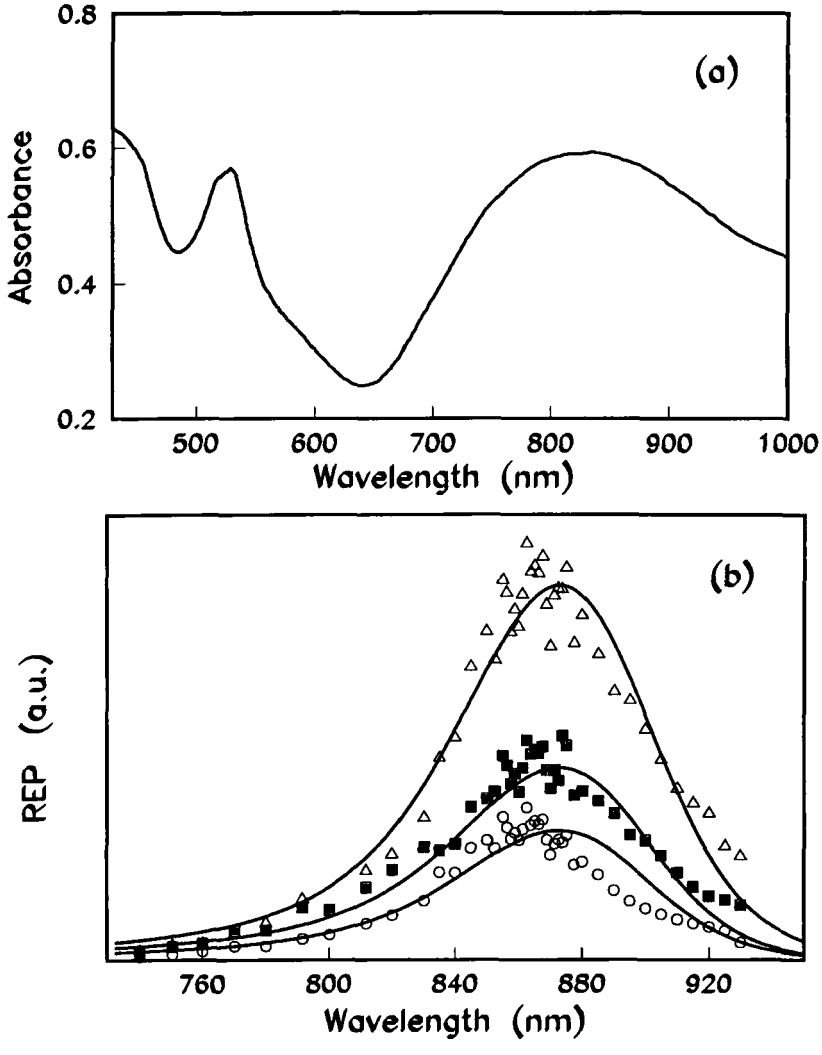

FIGURE 1 (a) Electronic absorption spectrum of $(TTF)_2(W_6O_{19})$ powders at 15 K. (b) Experimental (data points) and calculated (full curves) REPs for the normal modes at 55 (■), 90 (○) and 116 (△) cm^{-1} of a crystalline powder mixture of $(TTF)_2(W_6O_{19})$ and NH_4Cl at 15 K.

RRS spectra have been recorded with a multichannel triple spectrometer equipped with a CCD detector. A tunable (700 - 950 nm) Ti:sapphire laser pumped by an Ar^+ laser was used for excitation. Typical laser powers of 30 mW were employed. Measurements were performed at a nominal temperature of 15 K using a closed cycle helium refrigerator. The samples consisted of crystalline powder mixtures of $(TTF)_2(W_6O_{19})$ and NH_4Cl in a 1:130 weight ratio. The Raman band at 185.5 cm^{-1} of NH_4Cl was used as an internal standard for normalizing the measured intensities.

The electronic absorption spectrum of $(TTF)_2(W_6O_{19})$ measured on crystalline powders at 12 K is shown in Figure 1(a). The band at 530 nm is a localized excitation of the TTF^+ radicals whereas the broad band centered around 835 nm is attributed to the CT band of the $(TTF^+)_2$ dimers.

Figure 2 shows low frequency Raman spectra of the samples measured at various excitation wavelengths. The intensity enhancement of some bands when the excitation wavelength (λ_o) enters into resonance with the CT absorption band is made quite apparent by the comparison with the NH_4Cl band at 185.5 cm^{-1}. The spectrum obtained with λ_o = 530.9 nm, resonant with the localized excitation, is dominated by bands that do not undergo enhancement at resonance with the CT band and are mostly assigned to modes involving motions of the $(W_6O_{19})^{2-}$ anions [10].

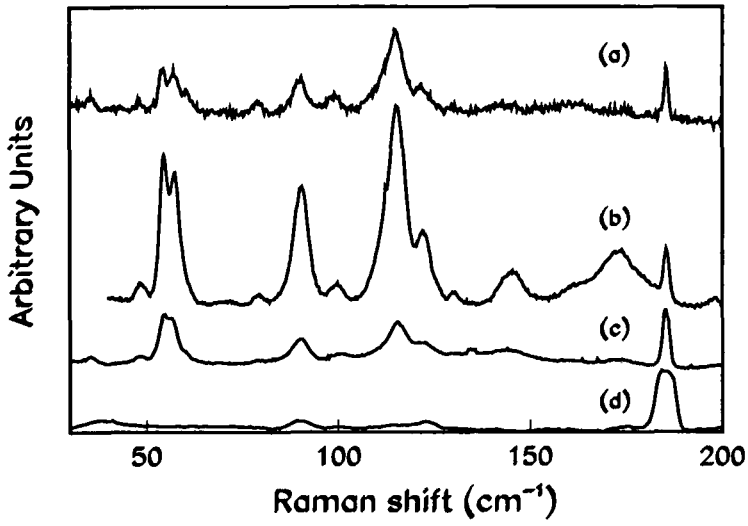

FIGURE 2 Raman spectra of a crystalline powder mixture of $(TTF)_2(W_6O_{19})$ and NH_4Cl at 15 K, obtained at different excitation wavelengths λ_0 : (a) λ_0 = 920.1 nm; (b) λ_0 = 860.0 nm; (c) λ_0 = 780.0 nm; (d) λ_0 = 530.9 nm.

Comparison (reported in detail elsewhere) of the frequencies and relative intensities observed in the Raman spectrum with λ_o = 860.0 nm with those

observed for (TTF)Br when the excitation wavelength (λ_o = 647.1 nm) yielding maximum enhancement of the Raman bands is used shows a striking similarity of the frequencies of the most intense bands in both compounds. The greater number of peaks observed for the bromide salt is quite understandable on account of the larger number of formula units per cell. If one recalls that the charges and especially the masses of the two counter–anions are very different ($MW[W_6O_{19}]$ = 1408 a.u.), these observations suggest that the modes of the $(TTF^+)_2$ dimers, notably those coupled to the CT band, are effectively decoupled from the other motion of the lattice.

The experimental Raman excitation profiles (REP) for the modes at 55, 90, and 116 cm^{-1} are reported as the data points in Figure 1(b). No clearly resolved vibronic structure is observable in the measured REP's which appear to be similar in shape to each other. Comparison with the structureless CT band absorption profile, shows that the REP's are narrower and peaked at a somewhat longer wavelength.

The absence of resolved vibronic structures can be understood as the result of the low frequency of the vibronically active intermolecular modes and of homogeneous bandwidths comparable to or greater than these frequencies.

A possible explanation of the observed mismatch between REP's and CT band, whose absorption profile extends to shorter wavelengths than the REP's, can be given in terms of the theoretically expected vibronic false origin induced by the HT coupling between states $|2\rangle$ and $|3\rangle$ via the intramolecular a_g modes.

The full curves are REP's calculated according to Eq. (9). All the terms in $|n^{HT}\rangle$, E^{HT} and the transition dipole matrix elements have been retained so that the calculated REP's account not only for the vibrational progressions originated by the linear diagonal EIP coupling but also for the frequency changes and Duschinsky rotations (quadratic EIP coupling) as well as for non–Condon (HT) contributions. The relative importance of the latter terms has been checked by deliberately omitting them from the calculation. It turned out that the non–Condon scattering channels indeed contribute significantly to the measured intensities.

An important feature of the calculation is its ability to account for the finite temperature effects. In fact the relative intensities of the REP's for the different Raman bands depend not only on the EIP coupling constants but also on the temperature through the Bose population factors contained in the equilibrium density matrix. A temperature of 25 K was chosen as a reasonable estimate of the effect of the local laser heating of the samples. However calculations performed for T = 40 K did not differ markedly.

The values of the parameters of the Peierls–Hubbard Hamiltonian used in calculating the REP's of Figure 1(b) are given below.

$$t = 0.27 \text{ eV} \quad ; \quad U = 1.05 \text{ eV}$$
$$\omega_1 = 66 \text{ cm}^{-1} \quad ; \quad \omega_2 = 94 \text{ cm}^{-1} \quad ; \quad \omega_3 = 122 \text{ cm}^{-1}$$
$$g_1 = 0.198 \text{ eV/Å} \quad ; \quad g_2 = 0.177 \text{ eV/Å} \quad ; \quad g_3 = 0.270 \text{ eV/Å}$$

A homogeneous width γ = 550 cm^{-1} is used for all the vibronic transitions. It should be noted that the frequencies used for the calculation are the "bare" ones

and do not coincide with those experimentally observed because of the "softening" due to the term in Eq. (8) quadratic in the matrix elements of H_{EV}.

The analysis of the optical spectra of a series of TTF halides reported by Torrance *et al.* [8] led to an estimate of $U \simeq 1.2$ eV and of $t \simeq 0.27$ eV, values in fairly good agreement with those we have adopted.

The values of the EIP coupling constants g_e ($e = 1,2,3$) reported above thus provide the first direct experimental estimates of such parameters. They substantially confirm that previous indirect estimates and results of theoretical calculations were in the correct range. An important merit of the RRS data compared with other spectroscopic measurements is their ability to single out the EIP coupled modes from the many lattice modes by way of their selective resonance enhancement. The identification of the coupled frequencies is thus independent of any attempt of assignment based, e.g., on lattice dynamical calculations, isotopic effects, polarization measurements. The suggestion of a substantial decoupling between intermolecular translational modes of the dimers and other unit cell motions given by the comparison of the results of $(TTF)_2(W_6O_{19})$ and of (TTF)Br deserves further investigation. If confirmed, it would encourage to assign some degree of generality to the coupling constants and frequencies of the EIP coupled modes reported here.

ACKNOWLEDGMENTS

Financial support by the Italian National Research Council (CNR) and by the Ministry of University and of Scientific and Technological Research is acknowledged. This work was developed under the "Progetto Finalizzato Materiali Speciali per Tecnologie Avanzate" of the CNR. We are grateful to M. Zanetti and L. Casagrande for technical help.

REFERENCES

1. T. Ishiguro and K. Yamaji, Organic Superconductors, (Springer–Verlag, Berlin, 1990).
2. R. Bozio and C. Pecile, in Spectroscopy of Advanced Materials, edited by R. J. K. Clark and R. E. Hester (John Wiley and Sons, Chichester, 1991), Chap. 1, pp. 1–86 and references therein.
3. R. Bozio, A. Feis, I. Zanon,and C. Pecile, J. Chem. Phys., 91, 13 (1989).
4. G.Fisher, Vibronic Coupling, (Academic Press, New York, 1984).
5. S. Hassing and O. S. Mortensen, J. Mol. Spectr., 87,1 (1981).
6. S. Mukamel, Adv. Chem. Phys., 70, Part I, 165 (1988).
7. H. M. Lu and J. B. Page, Chem. Phys. Lett., 131, 87 (1986).
8. J. B. Torrance, B. A. Scott, B. Welber, F. B. Kaufman and P. E. Seiden, Phys. Rev. B, 19, 730 (1979).
9. D. Attanasio, C. Bellitto, M. Bonamico, V. Fares and P. Imperatori, Gazzetta Chimica italiana, 121, 155 (1991).
10. C. Rocchiccioli-Deltcheff, R. Thouvenot et M. Daddabi, Spectrochimica Acta, 33A, 143 (1977).